B. TECH. PROJECT REPORT

On

Heat Transfer Characteristics of Downward Facing Hot Horizontal Surfaces using Mist Jet Impingement

BY

Parantak Sharma (130003025)
Ashutosh Kr. Yadav (130003011)

DISCIPLINE OF MECHANICAL ENGINEERING
INDIAN INSTITUTE OF TECHNOLOGY INDORE
November 2016

Heat Transfer Characteristics of Downward Facing Hot Horizontal Surfaces using Mist Jet Impingement

A PROJECT REPORT

Submitted in partial fulfillment of the
requirements for the award of the degrees
of
BACHELOR OF TECHNOLOGY
in
MECHANICAL ENGINEERING

Submitted by:
Parantak Sharma (130003025)
Ashutosh Kr. Yadav (130003011)

Guided by:
Dr. Santosh K. Sahu

INDIAN INSTITUTE OF TECHNOLOGY INDORE
November 2016

CANDIDATE'S DECLARATION

We hereby declare that the project entitled **"Heat Transfer Characteristics of Downward Facing Hot Horizontal Surfaces using Mist Jet Impingement"** submitted in partial fulfillment for the award of the degree of Bachelor of Technology in 'Mechanical Engineering' completed under the supervision of **Dr. Santosh K. Sahu, Associate Professor** ,IIT Indore is an authentic work.

Further, we declare that we have not submitted this work for the award of any other degree elsewhere.

Parantak Sharma **Date-**

Ashutosh Kr. Yadav

CERTIFICATE by BTP Guide(s)

It is certified that the above statement made by the students is correct to the best of my/our knowledge.

Signature

Dr.Santosh K Sahu

Associate Professor,

Mechanical Engineering,

IIT Indore

Preface

This report on "Heat Transfer Characteristics of Downward Facing Hot Horizontal Surfaces using Mist Jet Impingement " is prepared under the guidance of Dr. Santosh K Sahu.

An experimental investigation has been carried out to find the heat transfer characteristics of a hot plate when it is impinged using Mist. We have conducted experiments to find the dependence of various parameters like Air and Water flow rate ratio, Nozzle to plate distance, Radial distance. A correlation has been made for heat flux ratio at spatial point to stagnation point and is found to be in good agreement with the other test data.

The results obtained from the present experimental study are presented in the tabular and graphical form.

Parantak Sharma(130003025)
Ashutosh Kr. Yadav(130003011)
B.Tech. IV Year
Discipline of Mechanical Engineering
IIT Indore

Acknowledgements

First and foremost, we would like to thank our guide Dr. Santosh K. Sahu for guiding us thoughtfully and efficiently throughout this project, giving us an opportunity to work at our own pace while providing us with useful directions whenever necessary. We would like to thank Avadhesh Kumar Sharma (PhD scholar) for his constant support and contribution throughout the project. We would also like to thank Mr. Mayank Modak and Mr. Saurabh Yadav for their invaluable support and guidance. We would also like to express gratitude towards the entire fluid mechanics lab staff and workshop members for helping us whole heartedly along the way.

The financial support provided by the **Council of Scientific and Industrial Research (CSIR)**, **Government of India New Delhi, India** is gratefully acknowledged.

We would like to take this opportunity to thank our fellow batch mates for being great sources of motivation and for providing encouragement throughout the length of this project.

Finally, we offer our sincere thanks to all other persons who knowingly or unknowingly helped us in completing this project.

Parantak Sharma (130003025)
Ashutosh Kr. Yadav (130003011)
B.Tech. IV Year
Discipline of Mechanical Engineering
IIT Indore

Abstract

An experimental investigation has been carried out under transient conditions to study the effect of heat transfer characteristics of mist jet impingement on steel foil (AISI-304) of thickness 0.15 mm. The initial surface temperature of the plate was maintained at 515^0C with the help of an AC transformer. The local heat transfer characteristics are estimated from the thermal images obtained from infrared thermal imaging camera (A655sc, FLIR System). The IR camera and the nozzle (0.5 mm diameter) are positioned on either side of the target plate. The variation in surface temperature has been acquired at 8 different spatial points. It has been observed as we move away from stagnation point surface heat flux decreases irrespective of nozzle to plate distance and flow rates of water and air. The maximum surface heat flux is achieved at stagnation point and is not affected by the change in nozzle to plate distance, Air and Water flow rates. Surface heat flux can be controlled by changing the flow rates of water and air.

Table of Contents

List of Figures

List of Tables

Chapter 1

INTRODUCTION

1.1General Background

Rapid cooling of a high temperature solid surface is called quenching. Quenching was first used when people immersed solid metal pieces into bath of water to increase the material hardness and enhance the material properties. Jet impingement is a specialized case of quenching using specialized nozzles. Cooling surface with an impinging jets is an attractive technique because of its high efficiency and unsophisticated hardware requirements. But liquid jet provide rapid quenching that sometimes lead to crack formations and provide uncontrolled cooling, so for moderate and controlled cooling mist jets are used.

Mist cooling is a type of heat transfer to a dispersed flow that occurs when dispersed droplets Impinge on a heated surface. The heat transfer characteristics of mist cooling are similar to those of a boiling curve; however, mist cooling is more complicated than boiling heat transfer because it is effected by additional parameters such as droplet behavior and air flow rate.

Cooling by a dispersed flow is classified into either "spray cooling" or "mist cooling" according to the atomization of the droplets. In spray cooling compressed water is atomized by the pressure at nozzle, while in mist cooling, the droplets are atomized by compressed air. Therefore, the size of droplets in mist cooling is smaller due to the atomizing effect of compressed air, and heat transfer is also increased by the air flow from a nozzle. In air-atomized spray, when a droplet touches the surface, it becomes deformed. Heat transfer by the conduction mode occurs from the hot surface to the droplet, and the droplet gets partially evaporated. Subsequently, the partially evaporated droplet is swept away by the superposed airflow on the plate. However, the cooling by air atomized spray is not sufficient for quenching operations, such as ultra-fast cooling of a hot thick steel plate. For such applications, air-atomized spray cooling needs to be further enhanced. Spray cooling is mainly used to increase the cooling rate. However, mist cooling can be used for moderate cooling by controlling the liquid portion of dispersed flow. These characteristics make it possible to widely utilize mist cooling in diverse industrial fields, including steel-making processes, heat removal from high-powered electronic equipment, and advanced turbine systems.

1.2 Application

Mist cooling offers an attractive alternative to uncontrolled rapid quenching for thermal processing of steels, particularly in continuous casting, forging and extrusion operation. With mist cooling, one can raise or lower the cooling rate by increasing or decreasing the amount of liquid in the mixture. Controlled cooling, as an important procedure of thermal-mechanical control processing technology, is helpful to improve the microstructure and mechanical properties of steel. In industries for heat transfer

efficiency and homogeneous cooling performance which usually requires a jet impingement with improved heat transfer capacity and controllability.

Hot-rolled or continuous-cast billets are cooled to a given temperature on cooling beds, and then delivered to the subsequent process. Cooling beds with greater cooling capacities permit more billets to be cooled per unit area, which, in turn, leads to an increase in overall mill productivity or a reduction in the space taken up by the cooling beds. For these reasons, various types of forced billet cooling are in wide use. These conventional forced cooling methods can be classified as follows: -

1) Intensive natural cooling by accelerating the mill ventilation and natural convection on cooling beds

2) Application of air jet against billets

3) Application of water spray against billets.

4) Immersion of billets in water tank.

Requirements for the forced billet cooling are as follows.

a) Necessary and adequate cooling capacity

b) Provisions against cracking or bending of billets by forced cooling

c) Stable operation of the equipment over a long period of time

d) Low equipment and low operating cost.

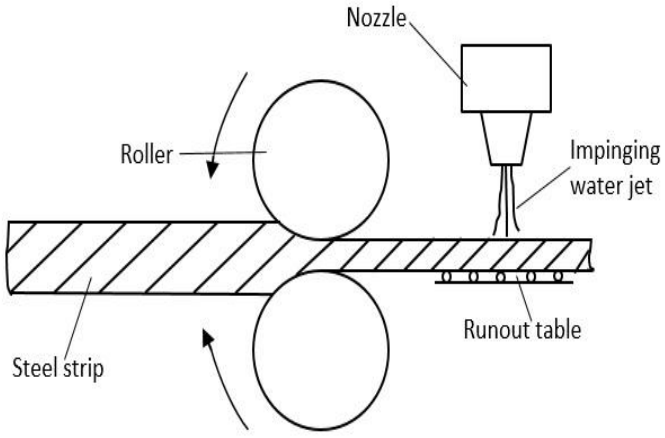

Fig.1.1-Hot steel strip mill cooling system [36]

The methods (1) and (2) satisfy the requirement (b), but not (a). The methods (3) and (4) satisfy (a), but, in many cases, not (b) and (c). The requirement (b) is supposed to be met by uniformly cooling billets over their entire surface and controlling cooling capacity, and the requirement c) by preventing nozzle clogging. So to meet all requirement of forced hot billets cooling, mist jet impingement is required as it provides controlled and moderate cooling.

Mist jet impingement cooling is a very efficient method for removing a large amount of heat from a uniformly heated surface. It has been applied widely to provide high heat transfer rates in many industrial processes, including the hardening and quenching of metals and tempering of glass. It is presently being explored for application to cooling of electronic components, nuclear fuel rods and space systems.

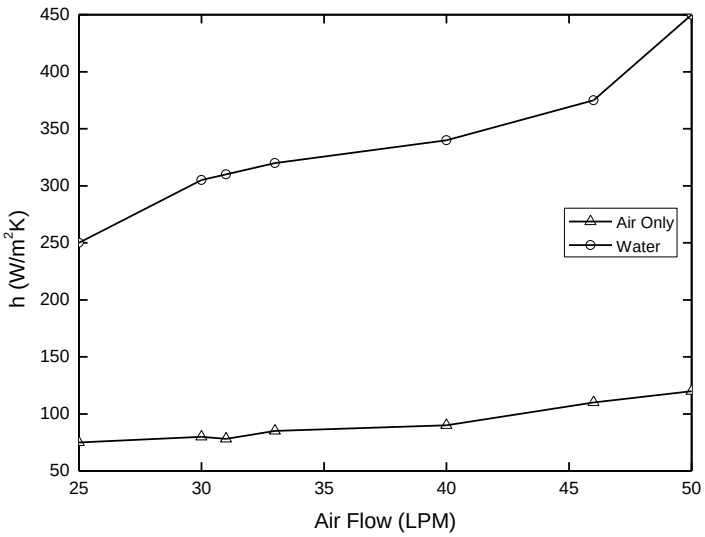

Fig.1.2-Comparison of heat transfer coefficient of air only
and mist jet impingement [37]

Heat fluxes of high end chips have already reached 150 W/cm^2 and are expected to rise rapidly in the future. It is now commonly accepted that the limits of air impinging jet are fast being approached for high-end applications, and the same limitation will be encountered for consumer applications soon.

1.3 Nozzle

Nozzles are used for three purposes: to distribute a liquid over an area, to increase liquid surface area, and create impact force on a solid surface. Nozzles can be categorized based on the energy input used to cause atomization, the breakup of the fluid into drops. Nozzles can have one or more outlets; a multiple outlet nozzle is known as a compound nozzle.

1.4 Types of nozzles

1. Single-fluid nozzle

Single-fluid or hydraulic spray nozzles utilize the kinetic energy of the liquid to break it up into droplets. This most widely used type of spray nozzle is more energy efficient at producing surface area than most other types. As the fluid pressure increases, the flow through the nozzle increases, and the drop size decreases. Many configurations of single fluid nozzles are used depending on the spray characteristics desired.

2. Two-fluid nozzles

Two-fluid nozzles atomize by causing the interaction of high velocity gas and liquid. Compressed air is most often used as the atomizing gas, but sometimes steam or other gases are used. The many varied designs of two-fluid nozzles can be grouped into internal mix or external mix depending on the mixing point of the gas and liquid streams relative to the nozzle face**.**

Types of Two-fluid nozzles

a- Internal-mix two-fluid nozzles

Internal mix nozzles contact fluids inside the nozzle; one configuration is shown in the figure below. Shearing between high velocity gas and low velocity liquid disintegrates the liquid stream into droplets, producing a high velocity spray. This type of nozzle tends to use less atomizing gas than an external mix atomizer and is better suited to higher viscosity streams. Many compound internal-mix nozzles are commercially used; e.g., for fuel oil atomization.

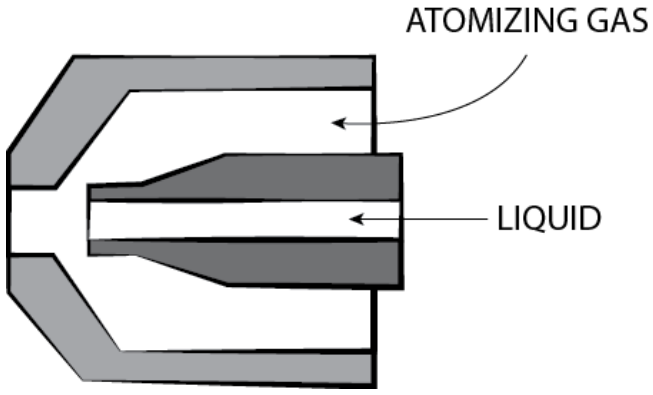

Fig.1.3-Internal mixing nozzle

b- External-mix two-fluid nozzles

External mix nozzles contacts fluids outside the nozzle as shown in the schematic diagram. This type of spray nozzle may require more atomizing air and a higher atomizing air pressure drop because the mixing and atomization of liquid takes place outside the nozzle. The liquid pressure drop is lower for this type of nozzle, sometimes drawing liquid into the nozzle due to the suction caused by the atomizing air nozzles (siphon nozzle). If the liquid to be atomized contains solids an external mix atomizer may be preferred. This spray may be shaped to produce different spray patterns. A flat pattern is formed with additional air ports to flatten or reshape the circular spray cross-section discharge.

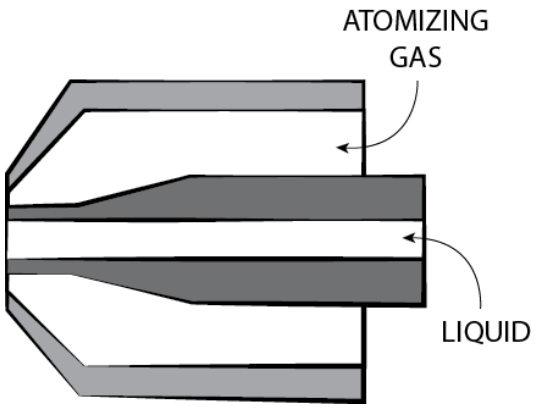

Fig.1.4-External mixing nozzle

1.5 Review of literature

When water mist cooling is applied to surfaces at low temperatures, nucleate boiling occurs. Many researchers have studied mist heat transfer at this condition. Typically, the recent ones are Graham and Ramadhyani [1], Lee et al. [2] and Yang et al. [3]. However, studies of mist impingement on surfaces at high temperature film boiling regime are limited. Pedersen [4] studied water droplets impinging upon a heated surface at 1800°F. His data of 200 to 400 mm droplets showed that the approaching velocity is the major parameter affecting droplet heat transfer and that surface temperature has minor effect on heat transfer. Choi and Yao [5] investigated an impacting spray experimentally. An impulse-jet liquid spray system and a solid particle spray system were compared. The effects of air convective were revealed. Nishio and Kim [6] reported the heat transfer of dilute spray impinging on hot surfaces. The report focused on the effects of the rebound motion and sensible heat of droplets on heat transfer in the high temperature region. A simple model was developed to predict the heat flux distribution of a dilute spray impinging on a hot surface. They assumed that the droplet number flow rate of the spray is small that the heat transfer of each droplet is independent.

Ideally, for the impaction cooling of water mist at high surface temperature, the heat transfer contribution of air and water could be separable and independent. An attempt was made by Deb and Yao [7], who modeled the spray cooling by considering droplet impingement heat transfer and air convective heat transfer

separately. The overall heat transfer is considered as the summation of these two contributions in addition to radiation cooling. However, no experimental verification was reported in terms of parametric study of these factors to validate this idea directly. In the present study, experiments were conducted on stainless steel disks at the high temperatures to verify these separable effects. Local heat transfer coefficients were measured in film boiling regime. The air flow and water flow are controlled independently and the operational conditions included pure air and water mist at different liquid mass fluxes. As a result, the air and water effects are revealed independently and parametrically. The Leidenfrost temperature was obtained at various air velocities and liquid mass fluxes. Sozbir and Yao [8] investigated a water mist cooling for glass tempering experimentally. Very high velocity air jet impingement was applied during the cooling process of glass tempering. The heat transfer of multiple water mist jets on glass was studied. The mist cooling demonstrates a definitive saving on the use of high-pressure air. When using mist cooling, the energy requirements of the system are significantly lowered.

With recent adoptions of closed-loop steam cooling by two major gas turbine manufacturers (Bannister and Little [9]; Mukavetz [10] for heavy-frame Advanced Turbine Systems (ATS), a major part of the external cooling load will be replaced by internal steam cooling. Generally, the internal heat transfer coefficient is required to be in the range of 8000; 10000 W/m2 K to replace the cooling load currently shared by external air-film cooling. Liquid water can achieve this goal easily, but problems with instability when boiling occurs have discounted its chances. With the availability of steam from the bottoming cycle of a heavy-frame ATS, mist/ steam cooling has been introduced by this research group as a potential means to significantly enhance the internal cooling of turbine airfoils. The advantages and reasons of using mist/steam cooling, a comparison of mist/air and mist/steam cooling, and a review of previous related studies have been presented by Guo et al. [10] and are not repeated here.

Basically, the concept of using mist/steam cooling to enhance cooling effectiveness is based on the following features discussed by Li et al. [11]: (a)single-phase heat transfer improved by increased mixing induced by particle dynamics, additional momentum and mass transfer induced by evaporation of liquid droplets on/near the wall, and increased specific heat, (b) the quenching effect of mist in the superheated boundary layer resulting in a steeper temperature gradient near the wall, and (c) the direct wallto- droplet heat transfer during impact releasing the latent heat of evaporation. Wachters et al. [12] considered the impact of droplets about 60 mm onto a heated surface at velocities in the range of 5 m/s. The investigation focused on identifying conditions under which impinging droplets would maintain the spheroidal state and the associated low rates of heat flow.

Goodyer and Waterston [13] considered mist/air impingement for turbine blade cooling at surface temperatures above 600°C. They suggested that the heat transfer was dominated by partial contact between the droplets and the target surface, during which the droplets vaporized at least partially. A vapor cushion and the elastic deformation of the droplets were responsible for rejecting the droplets. Addition of 6 % water

was found to improve the stagnation point heat transfer by 100 %, diminishing away from the stagnation point. Droplet size was found to have little effect for 30 mm, *d32,200* mm. Yoshida et al. [14] focused on the effect on turbulent structure with a suspension of 50-mm glass beads. In the impinging jet region, the gas velocity decreased due to the rebound of beads, accompanied by an increase in the normal direction velocity fluctuations. In the downstream region the effect was slight. The Nusselt number was found to increase by a factor of 2.7 for the relatively high mass flow ratios (solid/gas) of 0.8. Buyevich and Mankevich [15,16] modeled the particles in the mist as liquid discs separated from the wall by a vapor layer whose thickness is that of the wall roughness. A critical impact velocity was identified to determine whether a droplet rebounds or is captured. They applied the model to dilute mist impingement and reported agreement with experiment. Fujimoto and Hatta [17] studied deformation and rebound of a water droplet on a high-temperature wall. For Weber numbers of 10 to 60, they computed the distortions of the droplet as it flattened, contracted, and rebounded. They used a simple heat transfer model to confirm that surface tension dominates vapor production in the rebounding process. Hatta et al. [18] gave correlations of contact time and contact area of the droplet with Weber number.

Nirmalan et al. [19] conducted an experimental study of turbine vane heat transfer with water-air mist cooling. Water was pressured inside the vane and broken up into small droplets through many cooling holes on an inner wall inside the vane and impinged on the inner side of the vane's outer wall. Their results showed significant cooling enhancement using water/air mist jets, but they found the jets are difficult to control and resulted in non-uniform overcooling over the target surface. Guo et al. [11,20] studied the mist/steam flow and heat transfer in a straight tube under highly superheated wall temperatures. It was found that the heat transfer performance of steam could be significantly improved by adding mist into the main flow. An average enhancement of 100 % with the highest local heat transfer enhancement of 200 % was achieved with 5 % mist. Guo et al. [21] performed an experimental study on mist/steam cooling in a highly heated, horizontal 180° tube bend with the same experimental facility as above. Due to the effect of centrifugal force, the outer wall of the test section always exhibited a higher heat transfer than the inner wall. However, the inner wall exhibited higher heat transfer enhancement than the outer wall in most cases. The highest enhancement occurred at about 45° downstream of the inlet of the test section. The overall cooling enhancement of the mist/steam flow ranged from 40 % to 300 % with maximum local cooling enhancement being over 800 %.

Li et al. [22] reported results of a mist/steam slot jet impinging on a heated flat surface. They concluded that stagnation point heat transfer could be enhanced over 200 % by the addition of 1.5 % mist. The mist enhancement was found to decline to near zero by five slot widths downstream. Li et al. [23] compared the results of a slot jet and a row of discrete jets with equal mass flows. The comparison indicates that the slot achieves less cooling effectiveness in steam-only flow but produces superior cooling enhancement in mist/steam flow. If jet impingement cooling on turbine blades is employed, it is likely that the region will be

the inner surface corresponding to the external stagnation region (or leading edge of a blade). This region will have the highest amount of thermal challenge. The concave target surface will be characteristic of this region. A concave surface is known to cause flow instability within a boundary layer (Rayleigh [24]). Any fluctuation of fluid velocity will be amplified and result in more mixing. Studies have also been conducted on single-phase jet impingent with concave target surface.

Hrycak [25] studied heat transfer and flow characteristics of gaseous jets impinging on a concave hemispherical plate. He discovered that the total heat transfer on the concave surface is higher than that corresponding to a flat surface. Metzger et al. [26] conducted an experiment of impingement cooling on concave surfaces with lines of circular air jets. They reported that the lines of circular jets impinging on concaves surfaces produced higher heat transfer coefficients than comparable two-dimensional jets impinging on plane surfaces.

It is believed that the implementation of a fine water mist into the air stream has the potential to further increase the heat transfer rates. Indeed, Lee et al. [27] state that at droplet diameters of 30-80μm, a "superbly effective cooling scheme" is present. Convective heat transfer coefficients can increase by up to 10 times, through evaporation of an "ultra-thin" liquid film (50-100μm). The dispersal of water droplets into an air flow can be characterised as either spray cooling or mist jet cooling. A spray is obtained by pressurizing the water in the nozzle in order to atomize it. Mist jets use the air pressure to atomize the water. Mist jets thus allow smaller droplet size [28]. The liquid flow can be controlled with less atomization constraints.

Table 1.1-Studies on mist with different parameters

Author	Nozzle	Pressure MPa	Q_{air} ($\times 10^{-3}$) m^3/s	Q_w ($\times 10^{-5}$) m^3/s	T_p ^0C	Test Specimen	Remarks
Mohapatra et. al. [30]		P_w=0.08-0.14 P_{air}=0.2-0.4	0.5-5	1.7-4.1	400, 600, 900	AISI-1020 Steel (100*100*12)	Surfactant-SDS Surfactant Is added to water which increases spread-ability of water. Hence heat transfer increases.
Ravikumar et. al. [31]	Full cone atomizer at distance 60mm from plate		8.33	16.67	1050	AISI-304 Steel (100×100×6)	Surfactant-SDS, CTAB, Tween20
Agrawal et. al. [32]	At distance of 25 mm from plate	P_{air}=0.114	13.33	0.053	255 355 565	Stainless Steel (140×50×0.25)	Maximum surface heat flux largely depends on jet temp, jet flow rate or jet velocity.
Ravikumar et. al. [33]	170.801 (Lechler) At distance 60 mm from plate		8.33	16.67	900	AISI-304 Steel (100×100×6)	Surfactant-SDS,CTAB, Tween20
Jha et. al. [34]			8.33	20	1040	AISI-304 Steel (100×100×6)	Nano-fluid-Al_2O_3+SDS Nano-fluid helpful to break up the formation of vapour layer between the droplet and the plate surface.
Woei et. Al [35]	Distance 4W,6W 8W,10W						Mass flow rate of air-0.00496kg/s Mass flow rate of water-0.037-0.08kg/s

1.6 Scope of Dissertation

1. Mist jet impingement cooling of downward facing hot surface has not been extensively studied in the literature.
2. Very less studies recorded the effect of nozzle to plate distance on the heat transfer.
3. A few researcher have studied the effect of different flow rates of water and air.
4. No clear idea regarding the effect of radial distance on surface heat flux.

Chapter 2

Heat Transfer Characteristics of Hot Horizontal Surfaces using Mist Jet Impingement

2.1 Introduction

The objective of the present study is to evaluate the heat transfer behavior of mist jet impingement cooling. Here, a horizontal hot stainless steel thin plate is used as the test specimen. The thermal imaging technique is used to measure the surface temperature. Tests have been carried out for different value of air and water flow rates and for different nozzle to plate distance (15, 20, 25, 30 mm). A correlation determining the ratio of maximum heat flux at spatial point to maximum heat flux a stagnation point is proposed by using the experimental results and some significant observation are presented and discussed.

2.2 Experimental Setup and Procedure

2.2.1 Test facility

The schematic view of the test facility developed for the present investigation is shown in Figure 2.2. The test facility consists a test specimen, power supply system, and fluid supply system and instrumentation scheme for measuring the temperature of the test specimen. A smooth matt finish stainless steel (AISI-304) foil has been used as the test specimen in this study. The foil measures 250 mm in length, 60 mm in width and 0.15 mm in thickness. The test specimen is clamped lengthwise between two copper bus bars (Figure 2.5). Here, 10 mm of the test specimen on the either side is sandwiched between the copper bus bars in order to maintain a firm grip to the test specimen. This provision also ensures the uniformity in the supply of electrical power across the ends of the stainless steel test specimen by reducing the thermal contact resistance. The complete assembly involving test specimen, copper bus bar is clamped between L-shaped aluminium frame. A Bakelite sheet of 5 mm thickness is used in between the cupper bus bar and the aluminium frame to avoid any short circuit during electrical heating. Teflon buses also used to avoid direct contact of bolts with the aluminium frame. After each set of experiments the test specimen is stretched using a stretching screw (Figure 2.5) to avoid the thermal expansion and contraction due to heating and quenching. A 3-axis gear box is used to provide movement to the mist nozzle. Further, this is used to adjust jet to plate distance during the experimentation. Power supply to the test specimen is provided by an AC auto-transformer (3ϕ AC, 24 volts, 400 amps). A digital multimeter (Meco, $0-20\pm0.5\%$ volts, 0-400 $\pm$ 0.5% amp) is used to measure the voltage drop and the current supply across the test specimen. A calibrated gear pump (Micro pump, Model: GJ-N27-DEELE) is used to feed water from the coolant storage tank to the test specimen and a compressor (Max pressure-12 bar Tank capacity -300 liters) with is used to supply air. The

water flow rate of the gear pump is controlled by controller (12VArduino-UNO control) and air flow rate is controlled by FRL unit (Techno make, capacity 0.16-0.86MPa) and both fluid mixed inside the nozzle. Here, Pneumatic atomizing internal mixing nozzle (Lechler 136.115.xx.A2) with full cone spray angle of 20^0 of 0.5 mm diameter is used as the impinging nozzle from the bottom side of the test specimen.

The IR thermal imaging camera (Make: FLIR®, Model: A655sc; uncooled micro-bolometer detector array) has an operational spectral band of 7.5-14.0 μm and is capable of measuring the temperature in the range of $0^oC - 2000^oC$ with a scanning rate of 200 frames per second. The IR camera, positioned on the top of the test specimen opposite to the impinging nozzle, is used to record the local temperature distribution on the test specimen. As the maximum Biot number in the lateral direction based on the test specimen thickness (δ =0.15 mm) is of the order of 0.0059 (<<0.1), lumped assumption will holds good and the temperature gradient in that direction could be assumed negligible. Initially, sample tests have been carried out to evaluate the temperature drop across the test specimen during transient state condition. The temperature drop was found to be less than 0.25°C. Therefore, the temperature measured by the thermal camera on the reverse side of the test specimen is considered to be the temperature of the side exposed to liquid coolant. It may be noted that, infrared camera reads the temperature that depends on the emissivity value of the surface of the test specimen. Therefore, it is necessary to calibrate the emissivity (ε) of the target test specimen. In view of this, a test foil (250 mm × 60 mm × 0.15 mm) of stainless steel (AISI-304) was spot welded on the surface by one calibrated thermocouple (K-type) and painted with the heat resistant (flat black) paint on the other side for the uniform emissivity over the surface. The foil heated by using autotransformer and the electrical power supply is switched off once the plate temperature reaches to 530°C. Subsequently, the temperature of the foil decreases and the drop in temperature within 2.5 minutes is found to be 429°C. During this period, the thermal response of the test foil and the thermocouple readings are noted by using an infrared camera and Data Acquisitions System (Agilent Technologies, 34972A), respectively. Subsequently, suitable value of emissivity is fitted in the Research IR software to get the same temperature as read by the thermocouples. The procedure is repeated for various surface temperature of the test foil. The emissivity of the surface is found to be 0.95. The uncertainty in the temperature measurement is found to be $\pm 1.5^{\circ}C$.

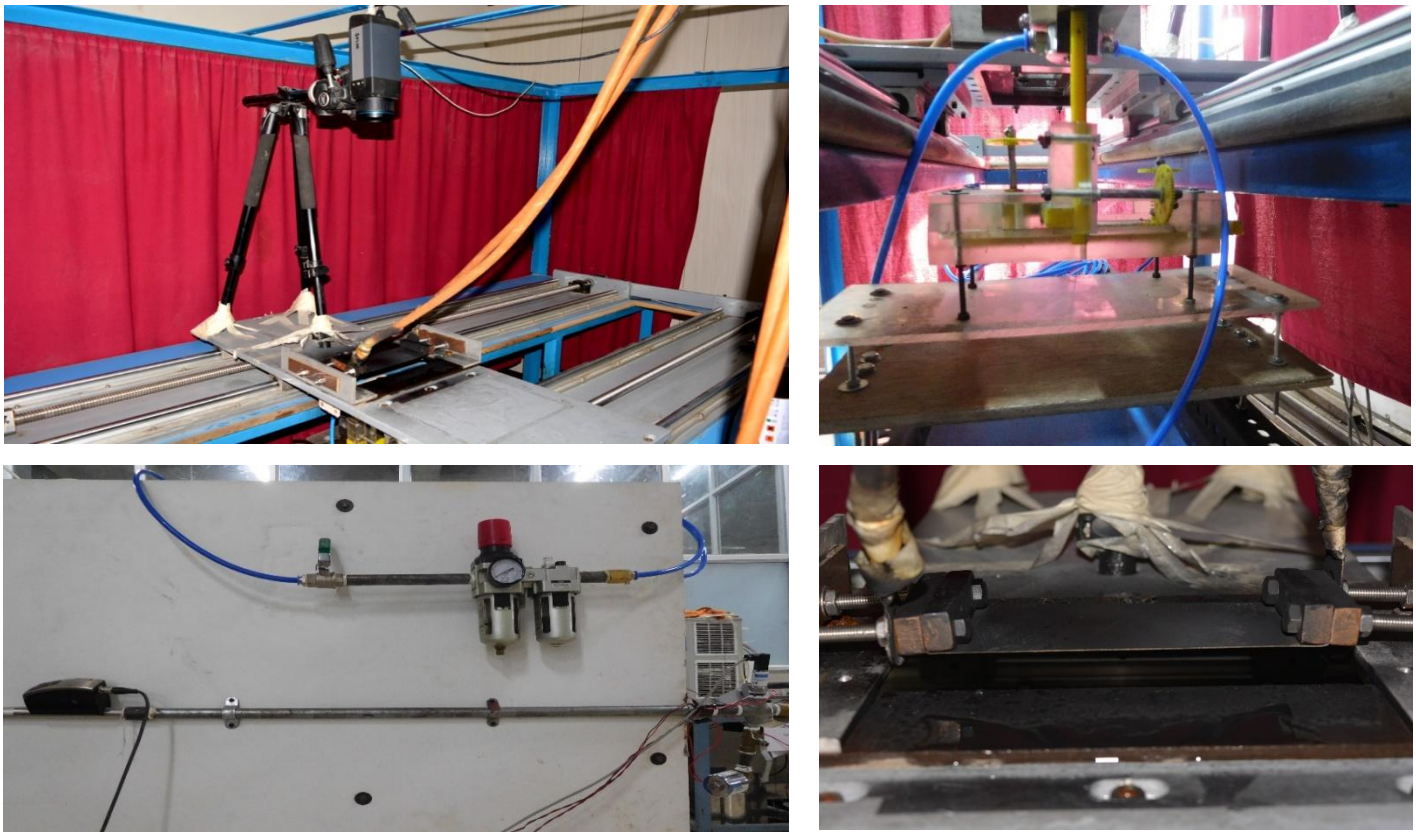

Fig.2.1- Photographic view of existing test facility

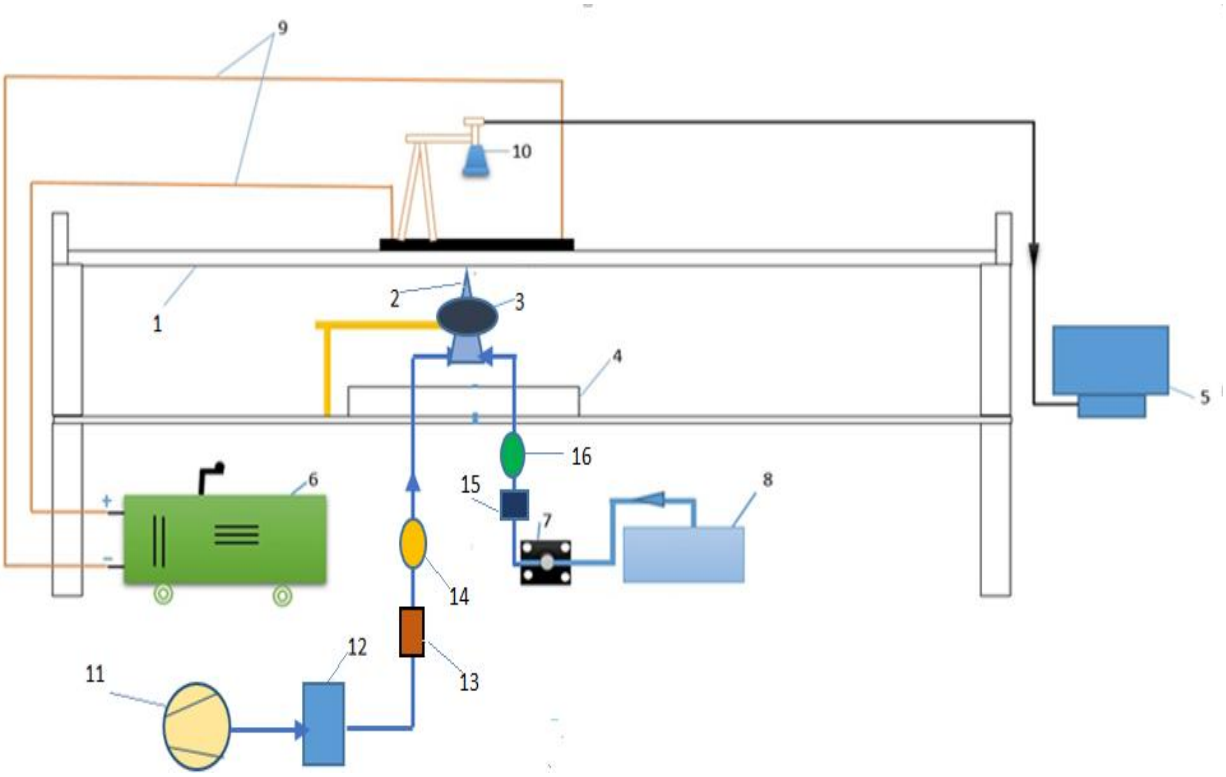

1	Table with stepper motor drive	9	Cables
2	Nozzle	10	IR camera
3	Nozzle adjuster	11	Compressor
4	Collecting tank	12	FRL unit
5	Personal computer	13	Air flow rate meter
6	Auto transformer	14	Air pressure gauge
7	Gear pump	15	Rotameter
8	Water tank	16	Fluid pressure gauge

Fig 2.2-Schematic view of test facility

2.2.2 Experimental procedure and data reduction

Tests are carried out at the atmospheric condition in the present investigation. Several parameters such as: emissivity of the target plate, distance of the target plate from thermal imager and scanning rate of the thermal imager are fixed and considered as input parameter in the experimental investigation (Table 2.3). The rotational speed of the gear pump is controlled by the controller to provide the desired flow rate of water and flow rate of air is controlled by FRL unit. Water is directed to flow through a 4mm internal diameter tube and air is directed to flow through 6mm internal diameter tube. The electric power to the target plate is supplied by an auto transformer under dry condition. During heating, the electrical power level are monitored by using a digital multimeter (Meco, 0-20 $\pm$ 0.5% volts, 0-400 $\pm$ 0.5% amp). After attaining the steady state condition, the power supply is switched off and the mist is allowed to impinge on the target plate through a nozzle (d= 0.5 mm) (table 2.5).

The thermal imager (A655sc, FLIR System) used in the present investigation is capable of measuring the temperature in the range of 0^0C -2000^0C with a scanning rate of 100 frames per second. Pixels are selected using the spot tool facility provided with the thermal imaging software. The rate of heat transfer (q) of the target plate under transient condition is assumed to be proportional to the temperature gradient and can be expressed as:

$$q = -\left(\frac{V}{A}\right)\rho c_p \frac{dT}{dt} \qquad (2.1)$$

Where, V is the volume of the material and A is projected area of the target surface, dT/dt is the change in temperature (T) of a given location with respect to time (t). In the present investigation, the initial temperature of the target surface was around 515^0C. The variation in various properties, namely, density (ρ) and specific heat capacity (c_p) are found to be negligible. Therefore, constant values of ρ and c_p are considered in the present analysis. The properties of the test specimen (AISI-304) are listed in Table 2.1. During experiments, three trial runs are conducted and the average is considered for further calculation. The range of operating parameters considered in the present experimental study is listed in Table 2.4. The temperature transients recorded by the thermal imager are used to evaluate the heat flux variation for varied range of operating parameters.

The present experimental study involves the measurement of various parameters, namely, length, width and thickness of the test specimen, diameter of nozzle, air and water flow rate, initial temperature of test specimen, initial temperature of air and water and time constant for temperature measurement by IR thermal imager and emissivity of the surface of test specimen.

Table 2.1 Dimension and thermo-physical properties of the test specimen

Material of test specimen	AISI-304
Area (A), mm^2	250x60
Thickness (δ), mm	0.15
Density(ρ), kg/m^3	8000
Specific heat capacity (Cp), J/kgK	500

Table 2.2 - Parameters used for the temperature measurement

Parameter	**Magnitude**
Image object parameters	
Emissivity ϵ	0.95
Reflected ambient temperature	32 ^{0}C
Atmospheric parameter	
Atmospheric temperature	28±2 ^{0}C
Relative humidity	0.55
Distance from IR camera to test specimen	0.5m
Transmission	0.99
IR Camera parameters	
Temperature range	150-650 ^{0}C
Resolution	640×480 pixels
Scanning rate	100 fps
Distance between each pixel	0.35 mm
Focal length	24.6 mm

Table 2.3 Experimental parameters

Parameter	**Operating range**
Standoff distance(mm)	15, 20, 25, 30
Jet diameter(mm)	0.5
Initial plate temperature(^{0}C)	515±10
Air flow rate and air pressure	0.3-10 m^3/hr, 0.4-6 bar
Water flow rate and Water pressure	1.5-21 lit/hr, 0.7-4 bar
Coolant inlet temp(^{0}C)	28

Nozzle used for experiments is *Lechler Pneumatic atomizing nozzle (136.115.xx.A2)*(Fig 2.3) is a full cone internal mixing nozzle with spray angle of 20^0 . It has a central liquid passage, annular air passage(Fig 2.4) and air and water mixes inside the nozzle and due to shear forces , water breaks into fine droplets. Internal mixing nozzle is used for low viscosity fluid.

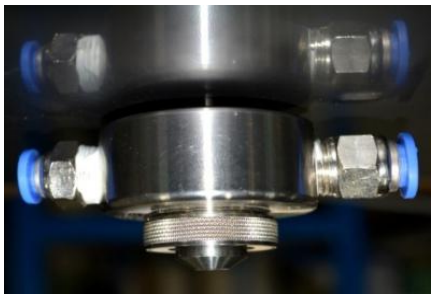

Fig 2.3-Nozzle

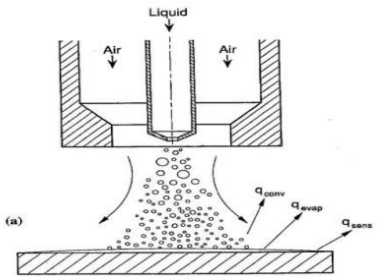

Fig 2.4 Schematic of mist jet[3]

Table 2.4 Characteristics of nozzle and dispersed flow under the experimental conditions

P_w(bar)	0.7	0.7	0.7	1.5	1.5	1.5	3	3	3	4	4	4
P_{air}(bar)	0.4	0.8	1.2	1.4	1.8	2.2	4	4.4	4.8	4.6	5	5.4
Q_w($\times10^{-5}$) (m^3/s)	0.163	0.105	0.047	0.161	0.114	0.061	0.081	0.056	0.031	0.152	0.114	0.081
Q_{air}($\times10^{-3}$) (m^3/s)	0.083	0.167	0.250	0.222	0.278	0.389	0.483	0.694	0.805	0.611	0.694	0.778
Q_w/Q_{air} ($\times10^{-2}$)	1.96	0.6	0.188	0.725	0.41	0.157	0.138	0.08	0.038	0.25	0.164	0.104

2.2.3 Thermal data and thermal image

A sample of the temperature transient data obtained during experimental study by using from the FLIR software is detailed below.

Table 2.5 Sample date sheet

Relative time	Sp1.Value	Sp2.Value	Sp3.Value	Sp4.Value	Sp5.Value	Sp6.Value	Sp7.Value	Sp8.Value
0	515.1741	504.2862	512.8269	507.8257	512.2113	516.2531	516.0202	519.4564
0.01	514.7445	503.7632	512.4083	507.4291	511.8047	515.8486	515.5789	518.9438
0.02	514.3393	503.4143	512.0511	506.871	511.6321	515.6525	515.0023	518.2964
0.03	514.0076	502.8033	511.6198	506.3995	511.1265	515.2231	514.855	518.0031
0.04	513.3314	502.7784	511.2375	506.3746	510.7934	514.8427	514.5604	517.3672
0.05	513.1714	501.9796	510.6453	505.9897	510.2378	514.413	514.1673	517.3672
0.06	512.8146	501.9047	510.2625	505.6791	509.8302	513.8232	513.8601	516.9144
0.07	512.6423	501.4925	509.8055	505.3933	509.3728	513.7863	513.3068	516.3511
0.08	512.1866	501.2175	509.4717	504.6969	509.1255	513.1469	513.1099	516.2408
0.09	511.7677	500.6548	509.3357	504.4854	509.0884	513.0361	512.6299	515.6893
0.1	511.3362	500.5422	508.8904	504.0123	508.8409	512.5068	512.5807	515.2599
0.11	510.9044	499.9915	508.4573	503.7133	508.2716	512.162	511.854	515.1741
0.12	510.4601	499.7411	508.2097	503.5887	507.6522	511.9525	511.4842	514.7077
0.13	510.2872	499.29	507.6274	502.8532	507.2555	511.3485	511.1018	514.2287
0.14	509.6448	498.6631	507.2431	502.8408	507.1439	510.9291	510.8551	513.8724
0.15	509.5706	498.475	507.1067	502.1919	506.5732	510.7934	510.4107	513.6142
0.16	508.9771	497.8851	506.4491	501.8048	505.9028	510.2131	509.9167	513.1838
0.17	508.6677	495.42	505.5797	501.155	505.6294	509.8919	509.447	512.7039
0.18	500.4922	466.3887	497.4957	498.2868	503.9874	508.5687	508.4573	511.9279
0.19	446.0009	419.1163	484.6581	493.8309	501.4175	506.3995	507.1439	510.6206
0.2	364.2119	371.8278	471.7196	489.5383	498.776	504.5476	505.1695	509.4594
0.21	248.3324	315.8398	460.6471	485.9993	496.5152	502.1045	503.6635	507.6646
0.22	167.6407	237.615	449.8663	482.1993	493.6667	500.1668	501.8298	506.1139
0.23	123.4838	180.6513	439.3227	478.8047	491.0734	497.86	499.7285	504.3235
0.24	99.56258	143.7753	428.8744	475.122	488.3945	495.5585	497.6088	502.6412

The data provided in the software was extracted on to excel sheets in the form of the sample illustrated above. Nodal analysis was carried out and the heat transfer characteristics were found out using the nodal analysis, using basic heat transfer equations. Origin Pro8.1 was used to plot the graphs.

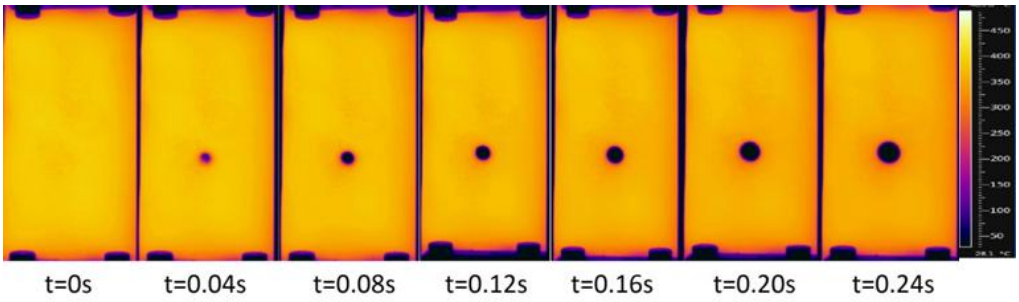

Fig 2.5 Thermal image of plate

Chapter 3

RESULTS AND DISCUSSIONS

3.1 Heat Transfer Characteristics of Hot Horizontal Surfaces using Mist Jet Impingement

3.1.1 Thermal image and cooling curves

Fig 3.1.shows the thermal image obtained by thermal camera (FLIR A655s) during the impinging jet cooling of the hot surface. The thermal images are recorded by using the thermal camera (FLIR A655sc) for a time step of 0.04 second and scanning rate of 100 fps. As it can be seen from the image that as the fluid strikes the hot surface its temperature drops from 500^0C to 60^0C in 0.04sec. It is observed that as time passes the stagnation zone grows and wet patch propagates in radial outward direction. Now further the temperature time transient history for the stagnation region for a given air pressure 0.8 bar and water pressure 0.7 bar and nozzle to plate distance (z=25mm) can be obtained by thermal image as depicted in Fig 3.1 using FLIR R&D software. The results are plotted for different water pressure and air pressure, different nozzle to plate distance and radial distance. From the Fig 3.2.three different zones can be observed during the cooling. Firstly from a-b small drop in temperature of the plate is observed. This is due to the cooling of the plate of due to natural convection. During b-c an immediate drop in the temperature of the plate occurs due to impingement of the mist on the surface of the plate. This section is followed by a constant temperature section c-d. However it is apparent form the Fig 3.2.that there is difference in slope for radial distance. The slope of the temperature distribution is higher at stagnation point on a given water and air pressure as compared to other spatial points in Fig.3.2. It can be observed that the temperature drop of the hot surface is rapid for high water flow rates.

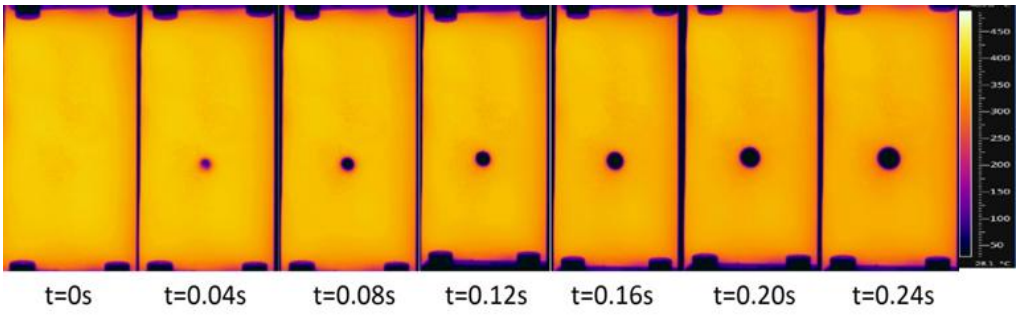

Fig 3.1 Thermal image of plate

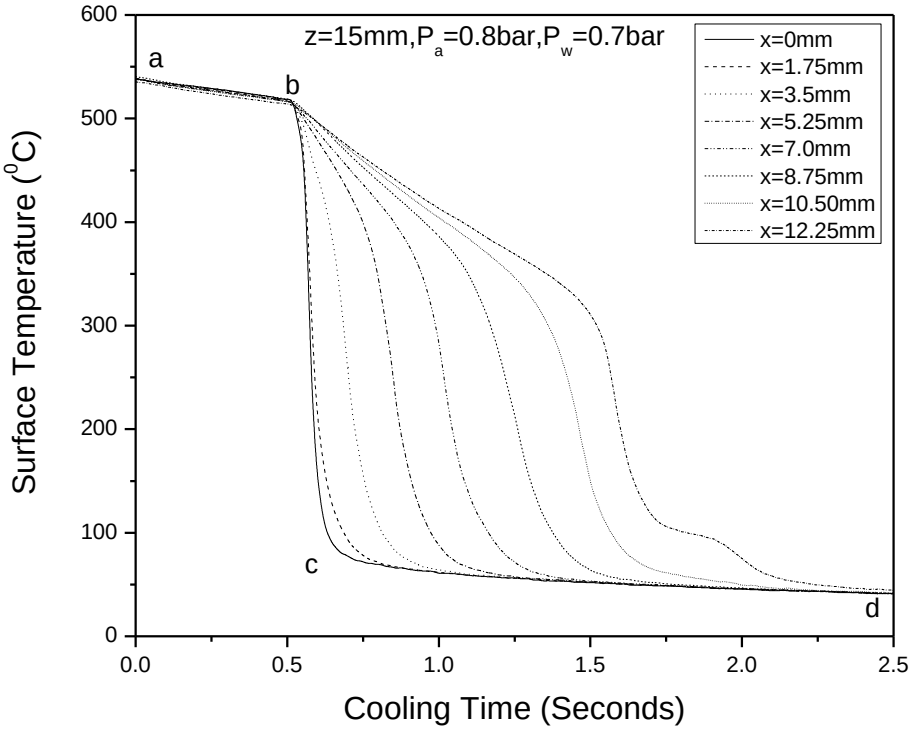

Fig 3.2 Temperature transients

(z=15mm, Pa=0.8bar, Pw=0.7bar)

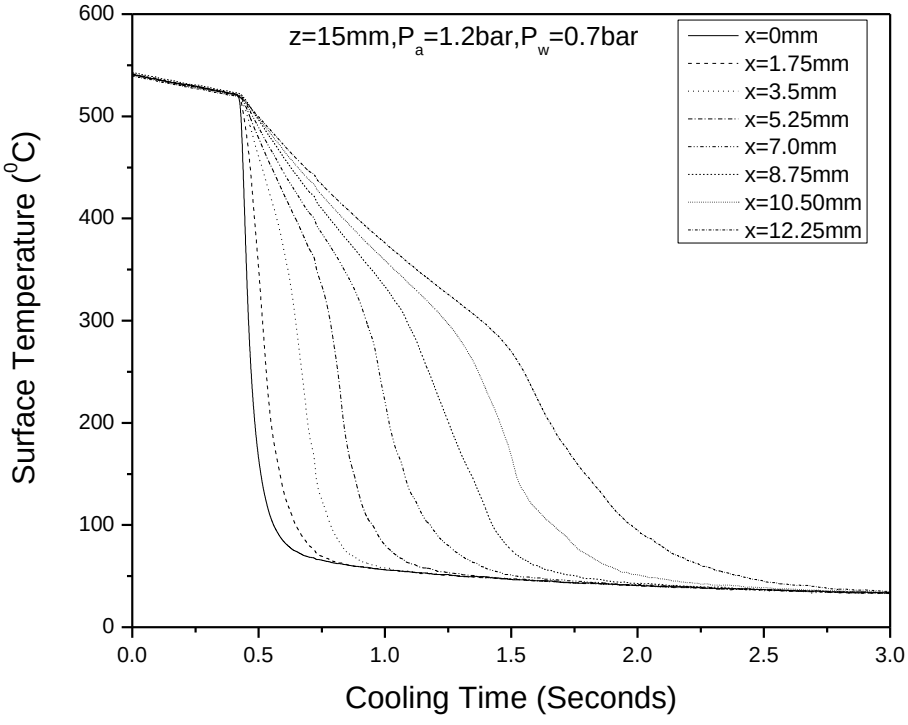

Fig 3.3 Temperature transients

(z=15mm, Pa=1.2bar, Pw=0.7 bar)

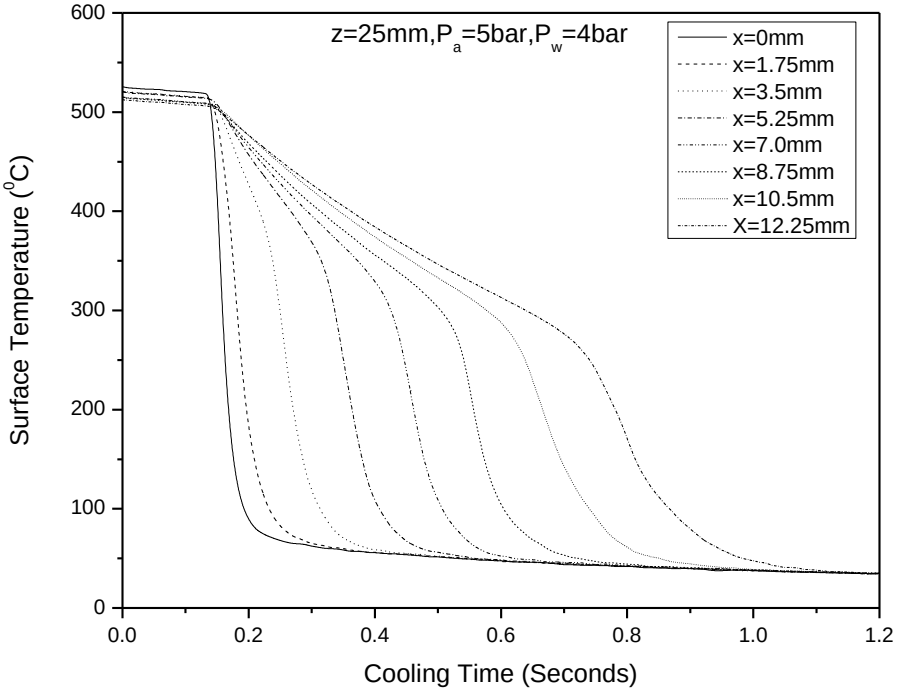

Fig 3.4 Temperature transients

(z=25mm, Pa=5bar, Pw=4bar)

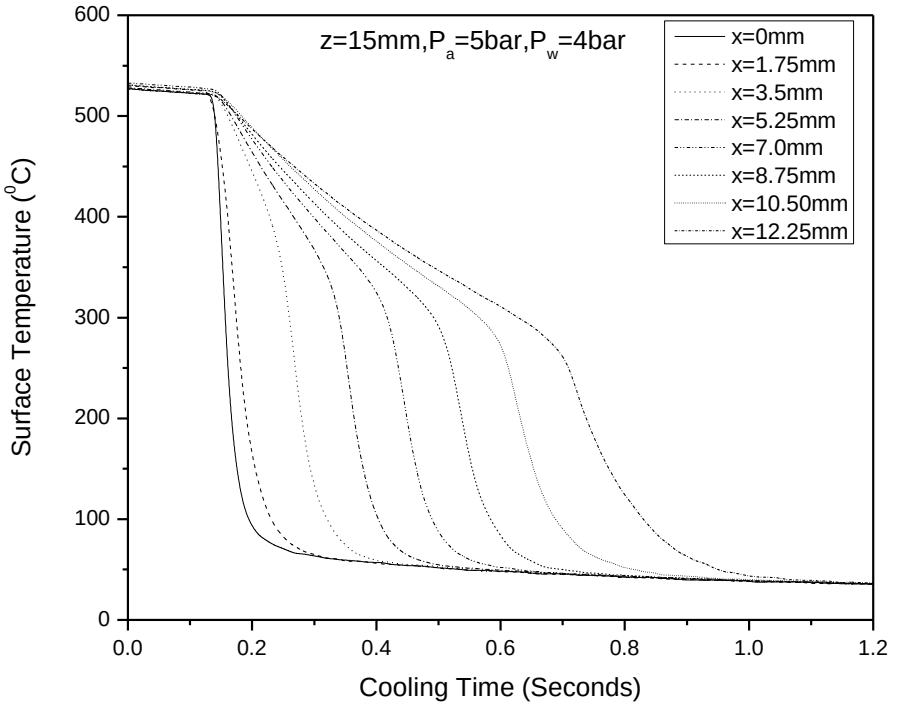

Fig 3.5 Temperature transients

(z=15mm, Pa=5bar, Pw=4bar)

3.1.2 Surface heat flux with time

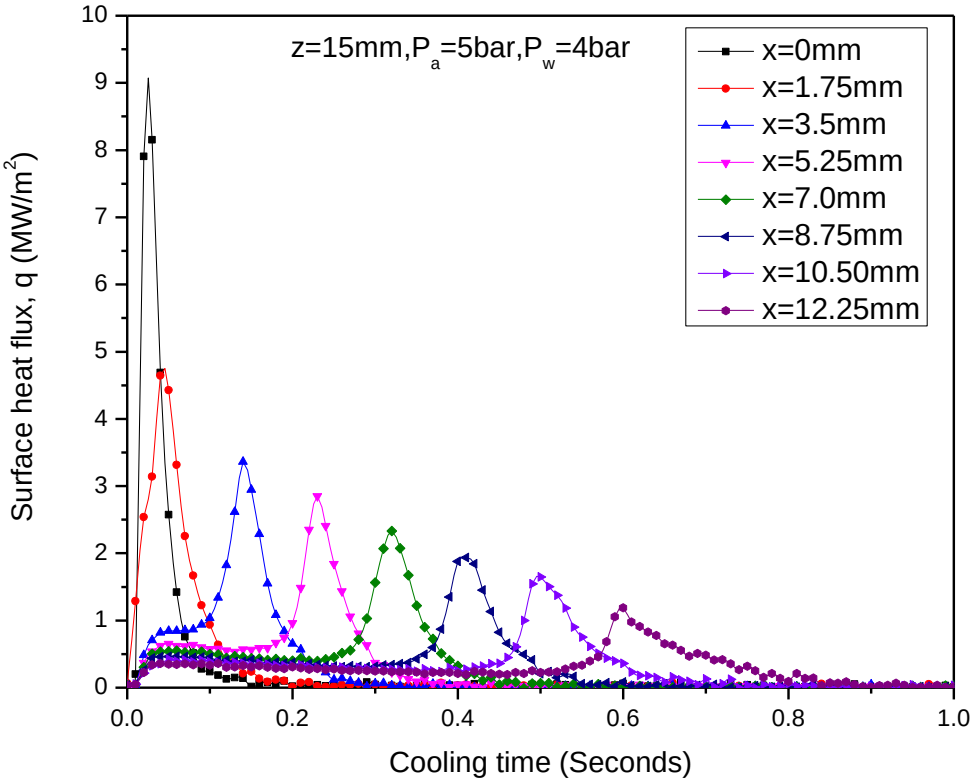

Fig.3.6 Surface heat flux with cooling time

($z=15mm$, $P_a=5bar$, $P_w=4bar$)

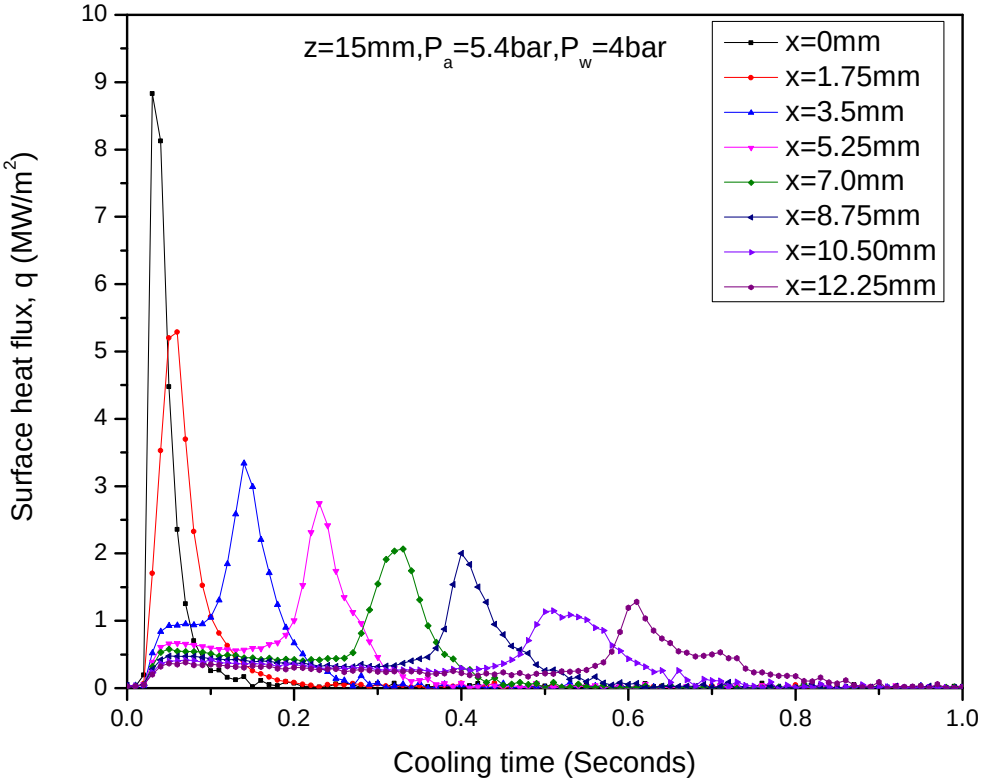

Fig.3.7 Surface heat flux with cooling time

($z=15mm$, $P_a=5.4bar$, $P_w=4bar$)

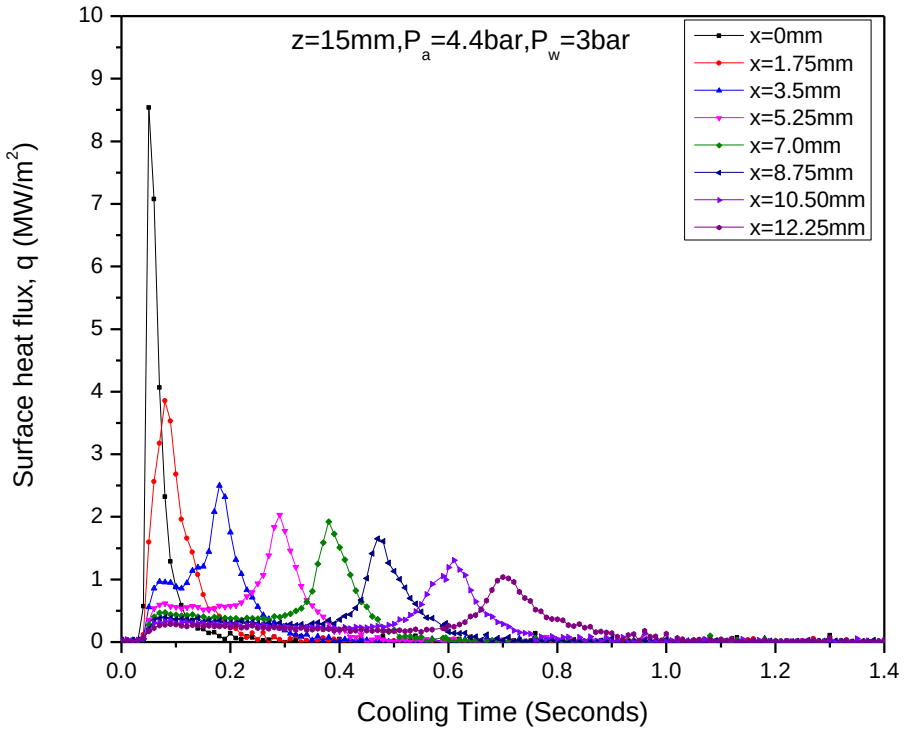

Fig.3.8 Surface heat flux with cooling time

($z=15mm$, $P_a=4.4bar$, $P_w=3bar$)

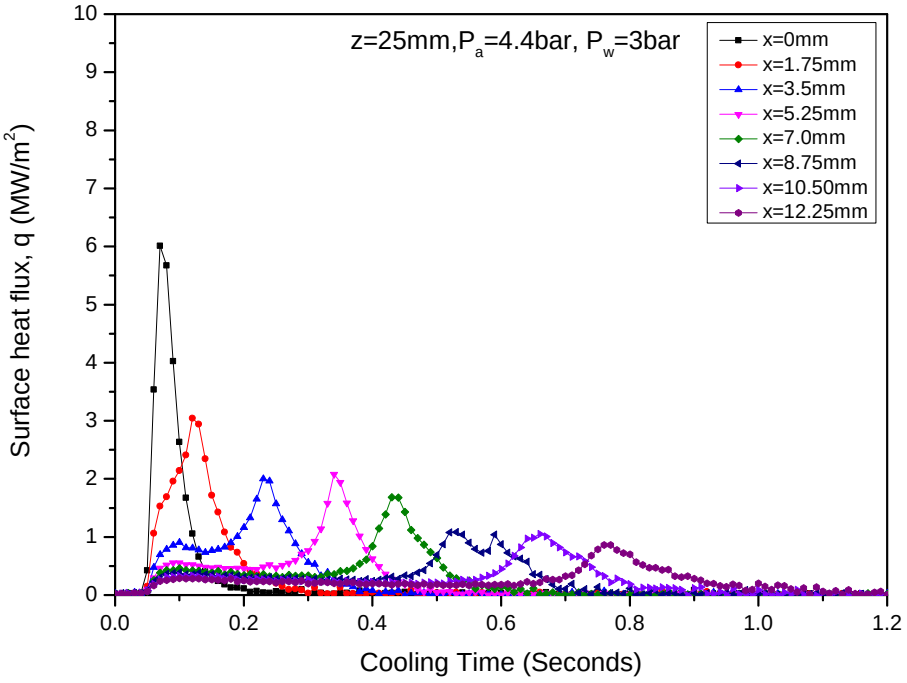

Fig.3.9Surface heat flux with cooling time

($z=25mm$, $P_a=4.4bar$, $P_w=3bar$)

The transient surface heat flux curves for different air pressure and water pressure at various spatial locations (0-12.25mm) are shown in Figures. It is observed in Figures, that at 515^0C initial surface temperature, the transient surface heat flux with the elapsed of cooling time initially increases and after attaining the peak it reduces monotonically. Such trend of change in surface heat flux with time is similar for the entire range of measured spatial locations. However, peak surface heat flux reduces substantially for other radial spatial locations. The rise in surface heat flux for stagnation point is sharp, whereas for other radial spatial locations the surface heat flux rises gradually. As nozzle to plate distance increases provided air pressure and water pressure remains constant, peak surface heat flux decreases at all spatial point in Fig3.8 & Fig 3.9. When nozzle to plate distance and water pressure remained constant but air pressure was increased, peak surface heat flux shows decreases because water flow rate decreases (Table 2.5) in Fig 3.6 & Fig 3.7.

3.1.3 Maximum surface heat flux with radial distance (effect of jet velocity)

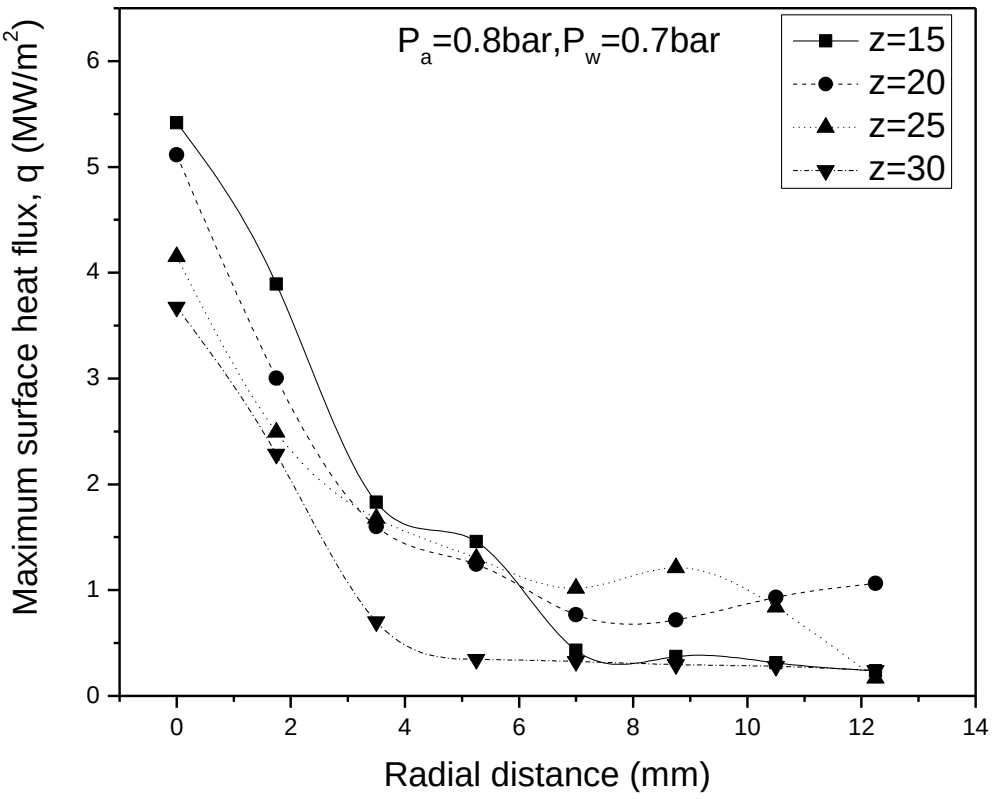

Fig.3.10 Surface heat flux with radial distance

(P_a=0.8bar, P_w=0.7bar)

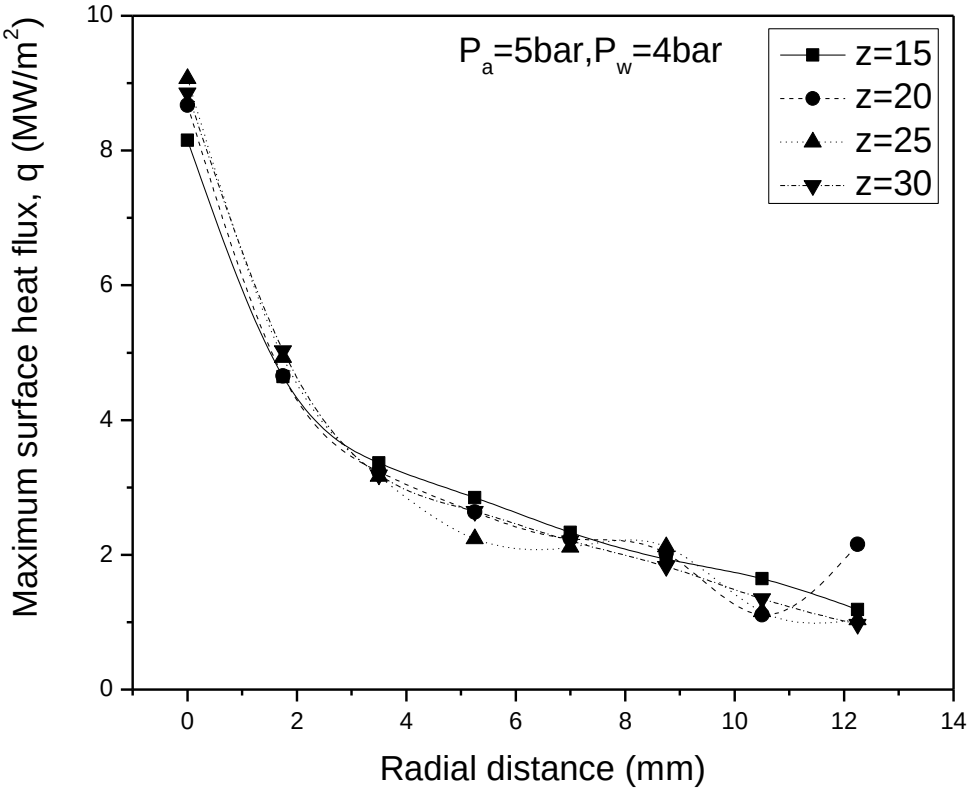

Fig.3.11 Surface heat flux with radial distance

(P_a=5bar, P_w=4bar)

The maximum surface heat flux for different nozzle to plate distance at various spatial locations (0-12.25mm) are shown in Figures. It is observed in Figures3.10, 3.11, maximum Surface heat flux is found maximum at stagnation point(x=0mm) and as we move away in radial outward direction, maximum surface heat flux decreases in Fig 3.10 & Fig 3.11. Jet velocity depends on air and water pressure. As water and air pressure increases, jet velocity increases and effect of nozzle to plate distance on maximum surface heat flux decreases because time take by mist to reach plate decreases as shown in Fig 3.10 & Fig 3.11(all trend lines are near to each other in Fig 3.11, where trends line are far to each other in Fig 3.10)

3.1.4 Maximum surface heat flux with radial distance (effect of air pressure)

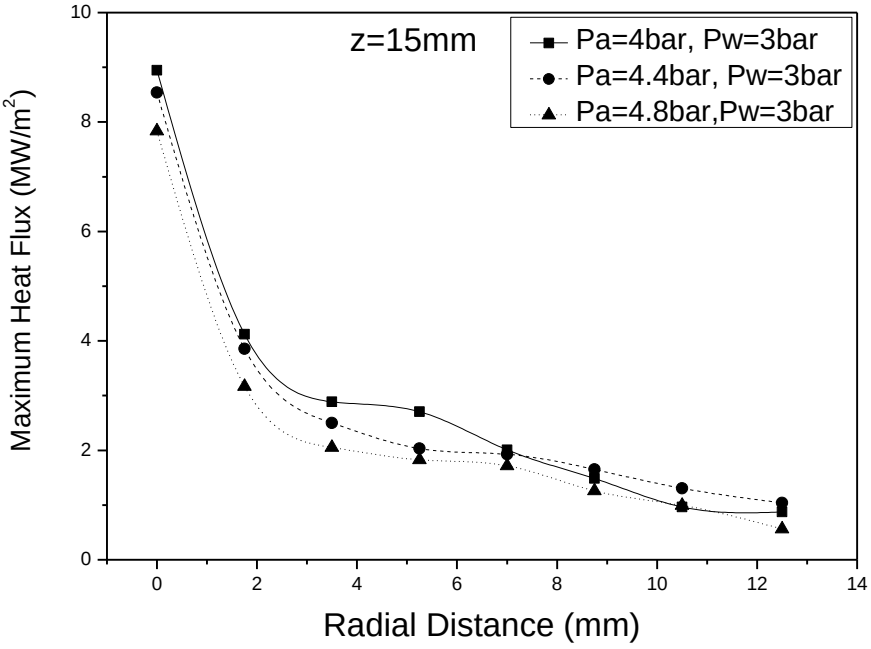

Fig.3.12 Surface heat flux with radial distance

(z=15mm)

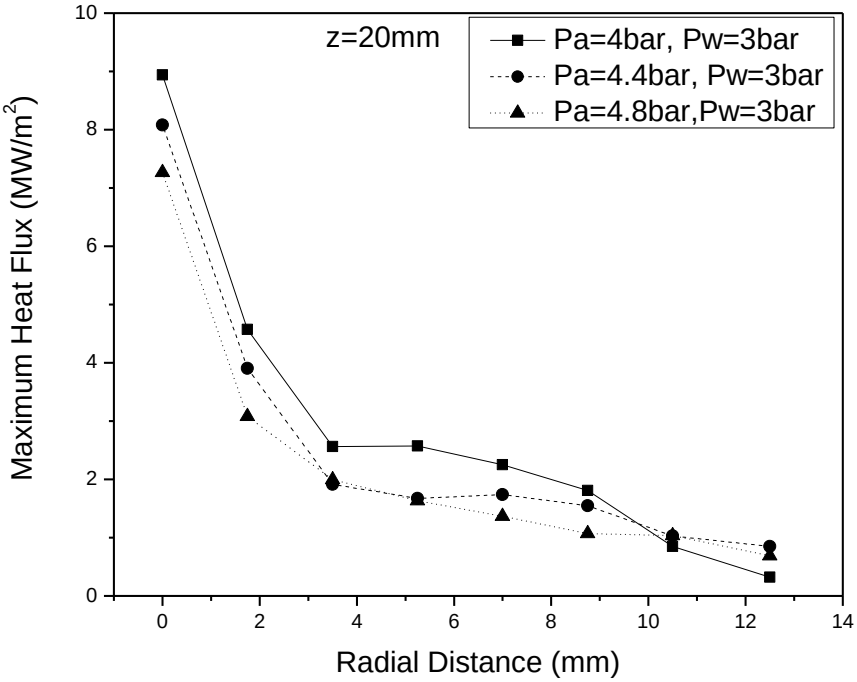

Fig.3.13 Surface heat flux with radial distance

(z=20mm)

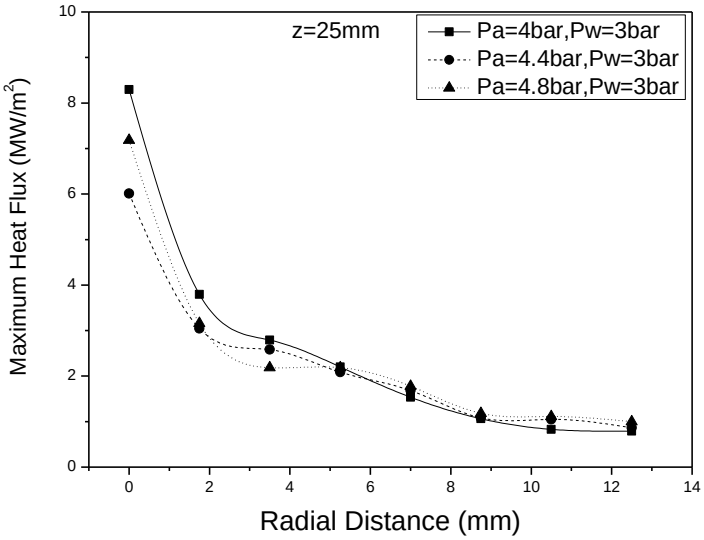

Fig.3.14 Surface heat flux with radial distance

(z=25mm)

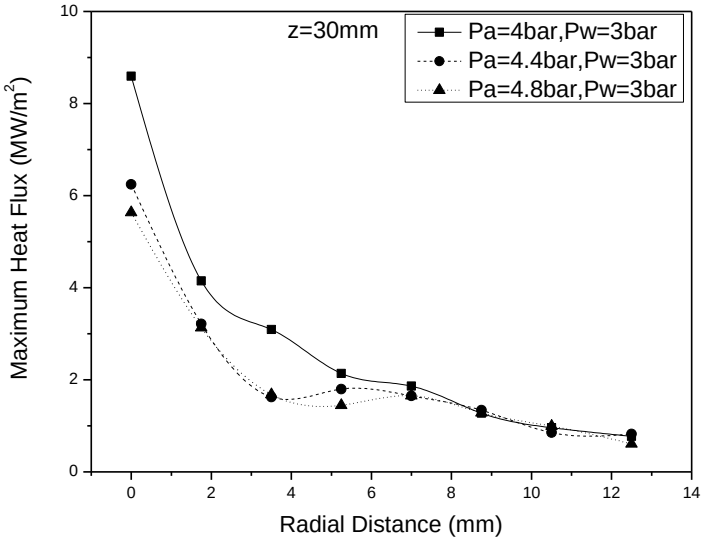

Fig.3.15 Surface heat flux with radial distance

(z=30mm)

The maximum surface heat flux for different nozzle to plate distance with different air pressure at various spatial locations (0-12.25mm) are shown in Figures3.12-3.15. It is observed in Figures3.12-3.15, as nozzle to plate distance increases, effect of air pressure increases. Difference of maximum heat flux at z=15mm with increasing air pressure is very low, and becomes significant when z=30mm.

3.2 Correlation

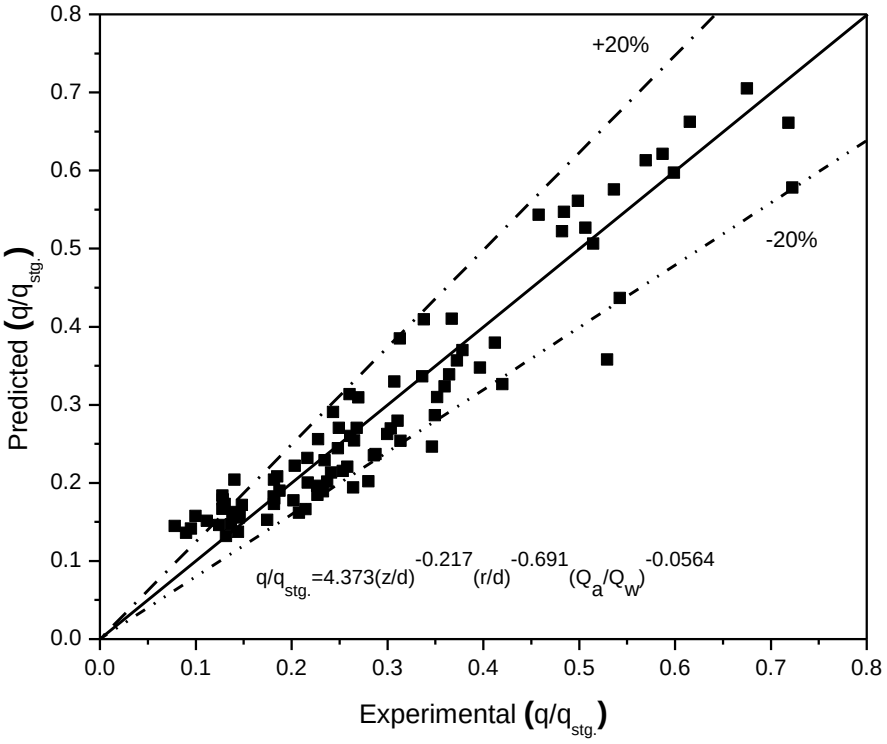

Fig 3.16 Comparison of experimental surface heat flux ratio with the proposed correlation for surface heat flux ratio

1. A correlation for the surface heat flux ratio ($^{q}/_{q_{stg.}}$) has been proposed as a function of various parameters such as: Flow rate ratio($^{Q_a}/_{Q_w}$), ratio of radial distance and nozzle diameter (r/d), ratio of nozzle to plate distance and nozzle diameter (z/d) and we got equation (3.1) for relation between these parameter.

$$\frac{q}{q_{stg.}} = 4.373\left(\frac{z}{d}\right)^{-0.217}\left(\frac{r}{d}\right)^{-0.691}\left(\frac{Q_a}{Q_w}\right)^{-0.0564} \quad \text{.....(3.1)}$$

2. The proposed correlation for ($^{q}/_{q_{stg.}}$)is able to predict the 80% of the test data within an error band of ±20%.

Chapter 4

CONCLUSIONS AND SCOPE FOR FUTURE WORK

4.1 Conclusions

An experimental investigation has been carried out to study the transient cooling of a horizontal hot surface using mist jet by bottom jet impingement. Tests have been performed to analyze the distribution of heat flux for a varied range of air and water flow rates, nozzle to plate distance (z=15, 20, 25,30mm) and surface temperature of 515^0C. The thermal imaging technique by using an infrared camera (A655sc, FLIR System) has been utilized to record the transient temperature during experiments. Following conclusions are made from the present experimental investigation and are detailed below

1. Experimental investigations have been performed to obtain surface temperature, surface heat flux and for a varied range of coolant flow rate of air and water and nozzle to plate spacing.
2. When the mist jet strikes on the stagnation point, a circular wet patch is formed in the stagnation region. The area of the wet patch increases with time and a distinct wet front is formed that found to propagate in the radial direction away from the stagnation point.
3. During transient cooling as the temperature gradient increases, the surface heat flux increases and attains its peak value, which corresponds to peak heat flux at that particular spatial location and time.
4. The peak surface heat flux is found to maximum at the stagnation point and reduces in the radial direction away from the stagnation point. The peak heat flux is highest at the stagnation point irrespective of flow rates and nozzle to plate distance.
5. Based on the investigation, a correlation has been proposed to predict ratio of surface heat flux as a function of various experimental parameters (Q_a/Q_w, z/d and r/d).

1.2 Scope for future work

1. To study heat transfer from different regions other than stagnation zone on a hot plate due to impingement of mist.
2. To study heat transfer behavior of mist jet impingement on hot horizontal moving plate.
3. To study heat transfer behavior of mist jet impingement on hot inclined plate.

Nomenclature

P Pressure

T Temperature

t Time

Q Flow rate of fluid

C_p Constant pressure specific heat

ρ Density

V Volume

A Area

q Heat flux

r Radial distance

d Nozzle diameter

z Nozzle to plate distance

Subscript

a air

w water

stg stagnation point

References

[1] Graham, K. M., and Ramadhyani, S., 1996, ‘‘Experimental and Theoretical Studies of Mist Jet Impingement Cooling,’’ ASME J. Heat Transfer, **118**, pp.343–349.

[2] Lee, S. L., Yang, Z. H., and Hsyua, Y., 1994, ‘‘Cooling of a Heated Surface by Mist Flow,’’ ASME J. Heat Transfer, **116**, pp. 167–172.

[3] Yang, J., Chow, L. C., and Pais, M. R., 1996, ‘‘Nucleate Boiling Heat Transfer in Spray Cooling,’’ ASME J. Heat Transfer, **118**, pp. 668–671.

[4] Pedersen, C. O., 1969, ‘‘An Experimental Study of the Dynamics Behavior and Heat Transfer Characteristics of Water Droplets Impinging upon a Heated Surface,’’ Int. J. Heat Mass Transf., **13**, pp. 369–380.

[5] Choi, K. J., and Yao, S. C., 1987, ‘‘Mechanisms of Film Boiling Heat Transfer of Normally Impacting Spray,’’ Int. J. Heat Mass Transf., **30**, pp. 311–318.

[6] Nishio, S., and Kim, Y. C., 1987, ‘‘Heat Transfer of Dilute Spray Impinging on Hot Surface—Simple Model Focusing on Rebound Motion and Sensible Heat of Droplets,’’ Int. J. Heat Mass Transf., **41**, pp. 4113–4119.

[7] Deb, S., and Yao, S. C., 1989, ‘‘Analysis on Film Boiling Heat Transfer of Impacting Sprays,’’ Int. J. Heat Mass Transf., **32**, pp. 2099–2112.

[8] Sozbir, N., and Yao, S. C., 2002, ‘‘Investigation of Water Mist Cooling for Glass Tempering System,’’ ASME International 6th Biennial Conference on Engineering Systems Design and Analysis (ESDA 2002), Istanbul, Turkey, July 8–11

[9] Bannister, R. L., and Little, D. A., 1993, ‘‘Development of Advanced Gas Turbine System,’’ Proc. of the Joint Contractor Meeting: FE/EE Advanced Turbine System Conference; FE Fuel Cells and Coal-Fired Heat Engine Conference, Aug., Morgantown, WV, pp. 3–15.

[10] Mukavetz, D. W., 1994, ‘‘Advanced Turbine System ~ATS! Turbine Modification for Coal and Biomass Fuels,’’ in Proceedings of the Advanced Turbine System Annual Program Review Meeting, Nov. 9–11, ORNL/Arlington, VA, pp. 91–95.

[11] Guo, T., Wang, T., and Gaddis, J. L., 2000, ‘‘Mist/Steam Cooling in a Heated Horizontal Tube, Part 1: Development of the Experimental Program,’’ ASME J. Turbomach., **122**, pp. 360–365.

[12] Li, X., Gaddis, J. L., and Wang, T., 2001, ‘‘Modeling of Heat Transfer in a Mist/Steam Impingement Jet,’’ ASME J. Heat Transfer, **124**, pp. 1086–1092.

[13] Wachters, L. H. J., Smulders, L., Vermeulen, J. R., and Kleiweg, H. C., 1966, ‘‘The Heat Transfer from A Hot Wall to Impinging Mist Droplets in The Spheroidal State,’’ Chem. Eng. Sci., **21**, pp. 1231–1238.

[14] Goodyer, M. J., and Waterston, R. M., 1973, ‘‘Mist-Cooled Turbines,’’ Conf. of Heat and Fluid Flow in Steam and Gas Turbine Plant, Proc. of Institution of Mechanical Engineers, pp. 166–174.

[15] Yoshida, H., Suenaga, K., and Echigo, R., 1988, ‘‘Turbulence Structure and Heat Transfer of A Two-Dimensional Impinging Jet with Gas-Solid Suspensions,’’ NHTC, **2**, pp. 461–467.

[16] Buyevich, Yu. A., and Mankevich, V. N., 1995, ‘‘Interaction of Dilute Mist Flow with a Hot Body,’’ Int. J. Heat Mass Transf., **38**, pp. 731–744.

[17] Buyevich, Yu. A., and Mankevich, V. N., 1996, ‘‘Cooling of a Superheated Surface with a Jet Mist Flow,’’ Int. J. Heat Mass Transf., **39**, pp. 2353–2362.

[18] Fujimoto, H., and Hatta, N., 1996, ‘‘Deformation and Rebounding Processes of a Water Droplet Impinging on a Flat Surface above Leidenforst Temperature,’’ ASME J. Fluids Eng., **118**, pp. 142–149.

[19] Hatta, N., Fujimoto, H., Kinoshita, K., and Takuda, H., 1997, ‘‘ExperimentalStudy of Deformation Mechanism of a Water Droplet Impinging on Hot Metallic Surfaces Above Leidenfrost Temperature,’’ ASME J. Fluids Eng., **119**,pp. 692–699.

[20] Nirmalan, N. V., Weaver, J. A., and Hylton, L. D., 1998, ‘‘An Experimental Study of Turbine Vane Heat Transfer with Water-Air Cooling,’’ ASME J. Turbomach., **120**~1!, pp. 50–62.

[21] Guo, T., Wang, T., and Gaddis, J. L., 2000, ‘‘Mist/Steam Cooling in a Heated Horizontal Tube, Part 2: Results and Modeling,’’ ASME J. Turbomach., **122**, pp. 366–374.

[22] Guo, T., Wang, T., and Gaddis, J. L., 2001, ‘‘Mist/Steam Cooling in a 180° Tube Bend,’’ ASME J. Heat Transfer, **122**, pp. 749–756.

[23] Li, X., Gaddis, J. L., and Wang, T., 2000, ‘‘Mist/Steam Heat Transfer of Confined Slot Jet Impingement,’’ ASME J. Turbomach., **123**, pp. 161–167.

[24] Li, X, Gaddis, J. L., and Wang, T., 2001, ‘‘Mist/Steam Heat Transfer of Circular Confined Impinging Jets,’’ ASME Paper 2001-GT-0151.

[25] Rayleigh, J. W. S., 1917, ‘‘On the Dynamics of Revolving Fluids,’’ Proc. R. Soc. London, Ser. A, **93**, Serial A, pp. 148–154.

[26] Hrycak, P., 1982, ‘‘Heat Transfer and Flow Characteristics of Jets Impinging on a Concave Hemispherical Plate,’’ Proceedings of the 7th International Heat Transfer Conf., **3**, pp. 357–362.

[27] Metzger, D. E., Yamashita, T., and Jenkins, C. W., 1968, ‘‘Impingement Cooling of Concave Surfaces with Lines of Circular Air Jets,’’ ASME Paper 68-WA/GT-1.

[28] Lee, S.L., Yang, Z.H. and Hsyua, Y., 1994, “Cooling of a heated surface by mist Flow“, Journal of Heat Transfer, Vol.116(1), pp. 167-172.

[29] Lee ,S., Park, J. , Lee, P. and Kim, M., 2005, "Heat transfer characteristics during mist cooling on a heated cylinder", Heat Transfer Engineering, Vol. 26(8) pp. 24-31.

[30] Mohapatra, S. S., and Jha, J. M. , 2013, "Enhancement of cooling rate for a hot steel plate using air-atomized spray with surfactant added water" A Journal of Thermal Energy Generation, Transport, Storage, and Conversion, pp.72-90.

[31] Ravikumar, S.V. and. Jha, J.M,2013, " Achievement of ultrafast cooling rate in a hot steel plate by air atomized spray with different surfactant additives" Experimental Thermal and Fluid Science pp.79-89.

[32] Agrawal, C. and Lyons, O.F. , 2013, " Rewetting of a hot horizontal surface through mist jet impingement cooling" International Journal of Heat and Mass Transfer pp. 188–196.

[33] Ravikumar, S.V., and Jha, J.M. ,2014, " Mixed surfactant additives for enhancement of air atomized spray cooling of a hot steel plate" Experimental Thermal and Fluid Science pp. 210–220.

[34] Jha, J.M., and Ravikumar, S. V. , 2015 "Ultrafast cooling of a hot moving steel plate by using alumina nano-fluid based air atomized spray impingement" Applied Thermal Engineering 738-747

[35] Chang, S.W., and SU, L.M. 2001, "Heat transfer of confined impinging air-water mist jet" JSME International Journal Vol. 44 No. 2 pp. 274-287

[36] Zumbrunen, D.A., Viskanta, R., and Incropera, F.P., 1989, “The effect of surface motion on Forced Convection film boiling heat transfer”, Transactions of the ASME, pp.760-767

[37] Oisinn, F.P., Lyons; Tim, Persoons; Gerard, Byrne, and Darina B., Murray, 2008, Water mist/air jet cooling of a heated plate with variable droplet size, Thermal issues in Emerging Technologies, ThETA 2, Cairao, Egypt, pp.-291-296.

Publications:

1. Ashutosh K. Yadav, Parantak Sharma, Avadhesh Kumar Sharma, Mayank Modak, Vishal Nirgude, Santosh K. Sahu, "Heat transfer characteristics of downward facing hot horizontal surfaces using mist jet impingement", 25th ICONE–International Conference on Nuclear Engineering, May 14-18, 2017, Shanghai Convention Center, Shanghai, China. **(Abstract Accepted)**
2. Avadhesh Kumar Sharma, Parantak Sharma, Ashutosh K. Yadav, Vishal Nirgude, Mayank Modak, Santosh K. Sahu, "An experimental investigation of transient cooling of hot horizontal surface by bottom jet impingement", 25th ICONE–International Conference on Nuclear Engineering, May 14-18, 2017, Shanghai Convention Center, Shanghai, China. **(Abstract Accepted)**